Lasers in Surgery and Medicine 37:138–143 (2005)

Determination of an Optimized Conversion Matrix for Device Independent Skin Color Image Analysis

Chang-Seok Kim, PhD,[1,2]* Moon Ki Kim, PhD,[3] Byungjo Jung, PhD,[4] Bernard Choi, PhD,[1] Wim Verkruysse, PhD,[1] Myung-Yung Jeong, PhD,[2] and J. Stuart Nelson, MD, PhD[1]

[1]*Beckman Laser Institute and Medical Clinic, University of California, Irvine, California 92612*

[2]*School of Nano Science and Technology, Pusan National University, Busan 609-735, Korea*

[3]*Department of Mechanical and Industrial Engineering, University of Massachusetts, Amherst, Massachusetts 01003*

[4]*Department of Biomedical Engineering, Yonsei University, Korea 220-710*

Background and Objective: A cross-polarized diffuse reflectance (CDR) color imaging system was developed for quantitative evaluation of port wine stain (PWS) response to laser therapy. To obtain calibrated Commission International de l'Eclairage (CIE) color space images from RGB (red, green, and blue) images, it was necessary to derive an optimized conversion matrix specific to our imaging system.

Study Design/Materials and Methods: A chromameter (CR-200, Minolta) and CDR imaging system were used to acquire CIELAB (CIE L^*, a^*, and b^*) tristimulus values and RGB image values, respectively. A cost function was defined using these sample data sets and then a minimization algorithm was applied to obtain an optimized conversion matrix for our imaging system and illumination conditions. CIELAB color space values (L^*, a^*, and b^*) obtained with the chromameter and CDR color images were compared to assess the accuracy of the derived matrix.

Results: In measurements using in vitro standard color patch or in vivo human skin samples, use of the optimized conversion matrix resulted in a good correlation with standard chromameter values for PWS human skin sites.

Conclusions: The cost function minimization algorithm resulted in an optimized conversion matrix for our CDR imaging system. Use of the optimized matrix improved the utility of CDR color image analysis as a simple non-contact measurement technique to monitor quantitatively PWS response to laser therapy. Lasers Surg. Med. 37:138–143, 2005. © 2005 Wiley-Liss, Inc.

Key words: port wine stain; skin color; CIE $L^*a^*b^*$

INTRODUCTION

Assessment of human skin color has become important in cosmetic science analysis and dermatologic diagnostics [1–4]. Since skin color perception is subjective in nature, objective color measurement systems such as scanning spectrophotometers [5], reflectance spectrometers [6], and tristimulus colorimeters [7] have been developed to measure color parameters quantitatively.

A portable handheld instrument, the tristimulus chromameter, based on the Commission International de l'Eclairage (CIE) L^* a^* b^* color space [8], is in popular use as a standard commercial reference device to measure skin color. Although the tristimulus colorimeter can provide quantitative measurement of skin color and detect color differences, its practical usefulness is limited due to: (1) the relatively small interrogation area; (2) inability to characterize an inhomogeneous surface appearance within the interrogation area; and (3) need for contact during the measurement [9]. The chromameter is typically assumed to provide a true measure of CIELAB color values.

An alternative method is to use a digital charged coupled device (CCD) camera-based system, which offers flexibility in selection of the interrogation area, relatively high spatial resolution, fast response time, and non-contact nature. However, the major problem of standard digital images is that the uncalibrated red, green, and blue (RGB) data depend on various device parameters such as camera settings, sensitivity, illumination conditions, and object position. The RGB values would change if a new flash lamp or CCD camera was used. In the long term monitoring of skin color dynamics, such a replacement would introduce an artifact and cause a discontinuity in the measurement data.

For a digital camera system to provide device-independent skin color values approaching those measured with the tristimulus chromameter, various calibration techniques have been applied to determine the system characteristics and transformation relationships [10–13]. The CIE 1976 (L^* a^* b^*) color space, or CIELAB, is commonly used as an absolute color scale for analysis of skin erythema, an important metric of hypervascular port wine stain (PWS) human skin. The RGB color space may be converted to

Abbreviations: PWS, Port Wine Stain; CIE, Commission International de l'Eclairage; CDR, Cross-polarized diffuse reflectance.

Contract grant sponsor: Arnold and Mabel Beckman Fellows Program; Contract grant sponsor: NIH grant; Contract grant numbers: AR47551, AR48458, EB002495.

*Correspondence to: Chang-Seok Kim, PhD, School of Nano Science and Technology, Pusan National University, Busan 609-735, Korea. E-mail: ckim@pusan.ac.kr

Accepted 21 June 2005
Published online 29 August 2005 in Wiley InterScience (www.interscience.wiley.com).
DOI 10.1002/lsm.20219

the CIELAB color space using a conversion matrix [1,2]. However, when the conversion matrix is not specifically optimized for a given imaging system [14,15], the converted color images may differ considerably from the standard CIELAB values and, therefore, would not allow comparison of images obtained under different measurement conditions or with those obtained by other investigators.

The purpose of the present study was to use a cost function minimization algorithm to derive an optimized conversion matrix specific to our cross-polarized diffuse reflectance (CDR) color imaging system to transform the device-dependent RGB color space into the device-independent CIELAB color space. As a practical example, we then applied the optimized method to quantitative analysis of PWS skin.

MATERIALS AND METHODS

Chromameter

The chromameter (CR-200, Minolta Co., Osaka, Japan) consists of a pulsed xenon arc lamp that illuminates the skin surface and collects the reflected light for tristimulus color analysis at 450, 560, and 600 nm. The instrument is positioned with minimal pressure perpendicular to the skin surface and CIELAB measurements are acquired over the 8 mm diameter interrogation area. A standard white plate is used to calibrate the instrument using a d65 illumination source [8]. As shown in Figure 1, the CIELAB color space is three-dimensional in nature. The achromatic luminance signal L^* represents the relative brightness from black (0) to white (+100). The chromatic parameter a^* represents the color spectrum from red (+) to green (−). A second chromatic parameter b^* represents the color spectrum from yellow (+) to blue (−) [15]. In the relatively homogeneous three-dimensional CIELAB color space, it is possible to compute a visual color distance between two sets of $L^*a^*b^*$ coordinates, ΔE^*, by calculating the Euclidean distance between the coordinate sets [3]. We can define the Euclidean distance from the origin, E^*, in the CIELAB space in Figure 1, as in Reference [9]:

$$E^* = \left[L^{*2} + a^{*2} + b^{*2}\right]^{1/2} \tag{1}$$

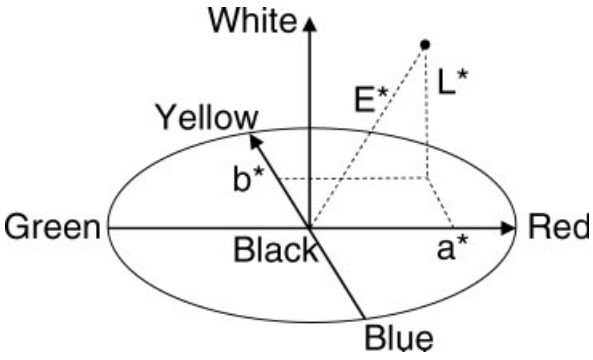

Fig. 1. Schematic of the three-dimensional CIELAB color space. E^* is the Euclidean distance from the origin.

CDR Color Imaging System

A color digital camera (Model DiMAGE7, Minolta Co., Osaka, Japan) was used to acquire RGB images with eight bits per color channel and sensor dimensions of 2560× 1920 pixels [15]. Environmental lighting and subject positioning conditions were controlled to ensure that sites were imaged in a reproducible manner. To address the effects of glare and non-uniform light illumination, two linear polarizers (Model A45-669, Edmund Industrial Optics, Barrington, NJ) were placed in front of both the camera lens and macro ring flash (Model 1200, Minolta Co., Osaka, Japan). The polarization axes were set to orthogonal states to reduce glare caused by specular reflectance from the skin surface [15]. A head-positioning device was mounted at a fixed distance from the digital color camera to ensure that facial skin sites were imaged in a reproducible manner [15]. The angle and height of the subject's head were adjusted to minimize artifacts induced by facial curvature [16].

In Vivo Color Measurements

Human data were acquired in accordance with a protocol approved by the Institutional Review Board at the University of California, Irvine. CIELAB and RGB values were acquired from 20 subjects with facial PWS currently undergoing laser therapy at the Beckman Laser Institute and Medical Clinic, and from 20 subjects with normal skin. Subject ethnicities were Caucasian, Asian and Hispanic. All 40 CDR RGB images were taken under the identical conditions of illumination, positioning, distance, and view angle. Skin sites that appeared homogeneous over an 8 mm diameter area were selected and RGB values averaged. Immediately after the CDR RGB images were acquired, the chromameter was used to measure skin color at exactly the same sites of 8 mm diameter area. Three consecutive measurements of CIELAB values per site were averaged for each chromameter measurement.

Conversion of Color Spaces

RGB values of each camera pixel were first converted into device-independent CIE XYZ tristimulus values using a 3× conversion matrix as shown in Equation (2) [1,2].

$$\begin{bmatrix} X \\ Y \\ Z \end{bmatrix} = \begin{bmatrix} p_1 & p_2 & p_3 \\ q_1 & q_2 & q_3 \\ r_1 & r_2 & r_3 \end{bmatrix} \begin{bmatrix} R \\ G \\ B \end{bmatrix} \tag{2}$$

XYZ images were converted into CIELAB color images using the following equation [8]:

$$\begin{aligned} L^* &= 116(Y/Y_n)^{1/3} - 16 \quad \text{if } Y/Y_n > 0.008856 \\ L^* &= 903.3(Y/Y_n) \qquad\quad \text{if } Y/Y_n \le 0.008856 \\ a^* &= 500[f(X/X_n) - f(Y/Y_n)] \\ b^* &= 200[f(Y/Y_n) - f(Z/Z_n)] \end{aligned} \tag{3}$$

where

$$\begin{aligned} f(t) &= (t)^{1/3} \qquad\quad \text{if } t > 0.008856 \\ f(t) &= 7.787(t) + 16/116 \quad \text{if } t \le 0.008856 \end{aligned}$$

and X_n, Y_n, Z_n are XYZ values of a reference standard.

For the CIELAB values measured with the chromameter, Equation (3) can be inverted to calculate XYZ values, as shown in Equation (4) [17]:

$$\begin{aligned}
Y &= Y_n f(Y/Y_n)^3 && \text{if } f(Y/Y_n) > (0.008856)^{1/3} \\
Y &= Y_n (f(Y/Y_n) - 16/116)/7.787 && \text{if } f(Y/Y_n) \le (0.008856)^{1/3} \\
X &= X_n f(X/X_n)^3 && \text{if } f(X/X_n) > (0.008856)^{1/3} \\
X &= X_n (f(X/X_n) - 16/116)/7.787 && \text{if } f(X/X_n) \le (0.008856)^{1/3} \\
Z &= Z_n f(Z/Z_n)^3 && \text{if } f(Z/Z_n) > (0.008856)^{1/3} \\
Z &= Z_n (f(Z/Z_n) - 16/116)/7.787 && \text{if } f(Z/Z_n) \le (0.008856)^{1/3}
\end{aligned} \tag{4}$$

Where

$$\begin{aligned}
f(Y/Y_n) &= (L^* + 16)/116 \\
f(X/X_n) &= a^*/500 + f(Y/Y_n) \\
f(Z/Z_n) &= f(Y/Y_n) - b^*/200
\end{aligned}$$

The performance of two conversion matrices was evaluated. The 3×3 conversion matrices $\mathbf{M_{r1}}$ and $\mathbf{M_{r2}}$ from References [1,2], respectively, have been used by other investigators [14,15], although these values were not specifically optimized to the respective measurement conditions. Using each matrix, our calculated CIELAB values from the 40 in vivo skin sites were compared with the values obtained using the chromameter. We anticipated that use of these non-optimized conversion matrices would result in relatively inaccurate CIELAB values.

Conversion Matrix Optimization

Using given sets of paired RGB and CIE XYZ values obtained with the CDR imaging system and chromameter measurements, respectively, a cost function was defined and then minimized to obtain an optimized conversion matrix for our system (Fig. 2) [10]. The cost function, C, is the discrepancy between the calculated and actual values. Assume a set of 1×3 row vectors to be $(\mathrm{RGB})_i$ and $(\mathrm{XYZ})_i$, where i, the number of vector pairs, is between 1 and n. To obtain the first row vector $\boldsymbol{p} = (p_1 \quad p_2 \quad p_3)$ of the conversion matrix in Equation (2), we define the least squares cost function, $C(\boldsymbol{p})$, in terms of the vector $\boldsymbol{p}$ based on the linear relationship between ith elements of RGB and ith element of X, as shown in Equation (5);

$$(\boldsymbol{p}) = \sum_{i=1}^{n} ((\mathrm{RGB})_i (p_1 \quad p_2 \quad p_3)^{\mathrm{T}} - X_i)^2 \tag{5}$$

The solution, which minimizes this function is

$$(p_1 \quad p_2 \quad p_3)^{\mathrm{T}} = K^{-1}\nu \tag{6}$$

where

$$K = \sum_{i=1}^{n} (\mathrm{RGB})_i^{\mathrm{T}} (\mathrm{RGB})_i$$

$$\nu = \sum_{i=1}^{n} X_i (\mathrm{RGB})_i^{\mathrm{T}}$$

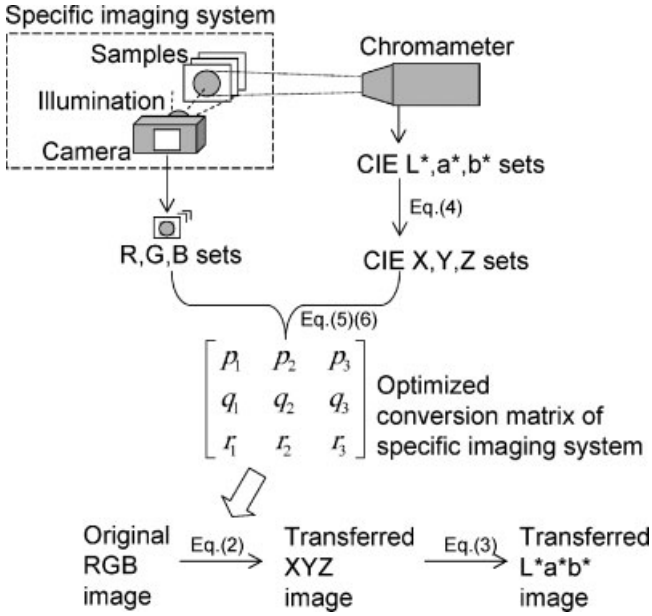

Fig. 2. Outline for deriving an optimized conversion matrix for our CDR imaging system and applying the matrix to obtain the corresponding CIELAB image.

Similarly, we can define cost functions for $q$and $r$given Y_i and Z_i, respectively, to acquire the optimized second and third row vectors, $(q_1 \quad q_2 \quad q_3)$ and $(r_1 \quad r_2 \quad r_3)$, respectively.

As input to the cost function minimization method, two approaches were studied. A Macbeth color checker (Gretag, New Windsor, NY) with 24 different color patch samples was used to derive an optimized conversion matrix, $\mathbf{M}_{\mathrm{patch}}$. RGB images and CIELAB chromameter values of each patch sample were obtained by the same procedures described above. Similarly, we derived a conversion matrix, $\mathbf{M}_{\mathrm{skin}}$, using 12 skin samples (6 PWS and 6 normal skin sites) selected from the 40 in vivo skin site measurements (20 PWS and 20 normal skin sites). From 20 PWS facial skin sites, the 6 samples with maximum and minimum values for each CIELAB value were selected, and the other 6 samples were similarly selected from 20 normal skin sites.

RESULTS AND DISCUSSION

Accuracy and Correlation of Conversion Matrices, $\mathbf{M_{r1}}$ and $\mathbf{M_{r2}}$

The CIELAB values measured with the chromameter and those calculated from the CDR imaging system measurements using the various matrices were compared to obtain the mean absolute difference, $<|\text{difference}|>$, and correlation coefficient, R, between the two sets of values. For PWS skin, the chromameter color value ranges were L^* (44.3–57.7), a^* (12.5–21.7), and b^* (5.9–17.1), and those of normal skin were L^* (52–64.5), a^* (10.9–17.5), and b^* (14.4–20.3), respectively.

TABLE 1. Performance Summary of Conversion Matrices, $\mathbf{M_{r1}}$ and $\mathbf{M_{r2}}$, to Compare Measured Chromameter CIELAB and E^* values with those Derived from RGB Images

	L^*		a^*		b^*		E^*	
	$<\|\text{difference}\|>$	R	$<\|\text{difference}\|>$	R	$<\|\text{difference}\|>$	R	$<\|\text{difference}\|>$	R
$\mathbf{M}_{r1}$	23.26	0.89	11.42	0.71	1.69	0.83	25.20	0.76
$\mathbf{M}_{r2}$	23.63	0.88	2.96	0.68	4.85	0.74	21.47	0.86

Here, $<|\text{difference}|>$ is expressed as the mean absolute differences between 40 sets of chromameter and derived CDR imaging values.

Using either $\mathbf{M}_{r1}$ [1,14] or $\mathbf{M}_{r2}$ [2,15], the mean absolute differences between the calculated $L^*a^*b^*$ values and the corresponding measured chromameter values were fairly large (Table 1). For example, the computed L^* value is 23 units higher than the measured chromameter value due to the brighter illumination of our CDR imaging system. These systematic shifts of color parameters also influenced R between both values. R also has a low value for the L^*, a^*, b^*, and E^* parameters. The correlation coefficients are reasonable, but are considerably less than those determined using the optimized matrix (Table 2). Figure 3a,b show the correlations between E^* parameters measured with the chromameter and the CDR imaging system using $\mathbf{M_{r1}}$ and $\mathbf{M_{r2}}$, respectively. The dotted lines are also plotted to represent a perfect match between the CDR system and chromameter, for reference.

Accuracy and Correlation of Optimized Conversion Matrix

The optimized matrices, $\mathbf{M}_{patch}$ and $\mathbf{M}_{skin}$, result in improved accuracy and R between our CDR imaging system and the chromameter values (Table 2). For example, the relation between E^* values by chromameter and those by CDR imaging system of $\mathbf{M}_{skin}$ is plotted in Figure 3c, which shows a high R value of 0.91 and a low $<|\text{difference}|>$ value of 1.49. This enhancement is due to matrix optimization related to the specific settings of our CDR system, which was treated as a black box in the cost function minimization process [10]. Using the derived conversion matrix $\mathbf{M}_{skin}$, the CDR imaging system color values become linked directly to those measured by the chromameter. This method has the advantages of simplicity and cost effectiveness compared to other system calibration methods [10–13], in that it is not necessary to verify the illumination conditions of each imaging component in the CDR system.

Comparing the results obtained using $\mathbf{M}_{patch}$ of 24 in vitro samples and $\mathbf{M}_{skin}$ of 12 in vivo samples, the latter matrix performs better with lower $<|\text{difference}|>$ and higher R for each CIELAB parameter of human skin, as shown in Table 2. We attribute this trend to the difference in light propagation within the color pastels versus in vivo human skin. Since skin is more scattering than color pastels, the remitted light distribution differs considerably from the diffusely reflected light. Photon diffusion in in vivo skin shows strong wavelength dependence [18]. Thus, by using in vivo skin sample measurements in the optimization process, this effect is inherently taken into account, resulting in better performance of $\mathbf{M}_{skin}$.

Image Analysis of Port Wine Stain Human Skin

With the optimized conversion matrix, $\mathbf{M}_{skin}$, we analyzed a RGB image of PWS skin in Figure 4a taken with our CDR imaging system. When the chromameter was used to measure the PWS color of this patient, the central region of the lesion had measured values of $L^* = 48.2$, $a^* = 17.4$, and $b^* = 11.7$; these were averaged color values of the apparently inhomogeneous PWS skin site. With the chromameter, it is not possible to measure color values in subregions of large PWS lesions. However, when the RGB values contained in the dashed box shown in Figure 4a were converted using the optimized conversion matrix, $\mathbf{M}_{skin}$, the images of L^*, a^*, b^*, and E^* in Figure 4b showed color value maps with higher spatial resolution and good correlation of the CIE $L^*a^*b^*$ parameters. By collecting CDR color images of PWS patients after several laser treatments, the color parameters can be used as a device-independent record of lesion response and therapeutic outcome [3]. Moreover, further image analysis can be performed to quantify the erythema, hemoglobin, and melanin content from the skin color information [15,18].

TABLE 2. Performance Summary of Optimized Conversion Matrices, $\mathbf{M_{patch}}$ and $\mathbf{M_{skin}}$, to Compare CIELAB and E^* values with those Derived From RGB Images

	L^*		a^*		b^*		E^*	
	$<\|\text{difference}\|>$	R	$<\|\text{difference}\|>$	R	$<\|\text{difference}\|>$	R	$<\|\text{difference}\|>$	R
$\mathbf{M}_{patch}$	5.78	0.88	2.71	0.68	1.92	0.83	5.83	0.81
$\mathbf{M}_{skin}$	1.52	0.91	1.61	0.77	0.90	0.94	1.49	0.91

Here, $<|\text{difference}|>$ is expressed as the mean absolute differences between 40 sets of chromameter and derived CDR imaging values.

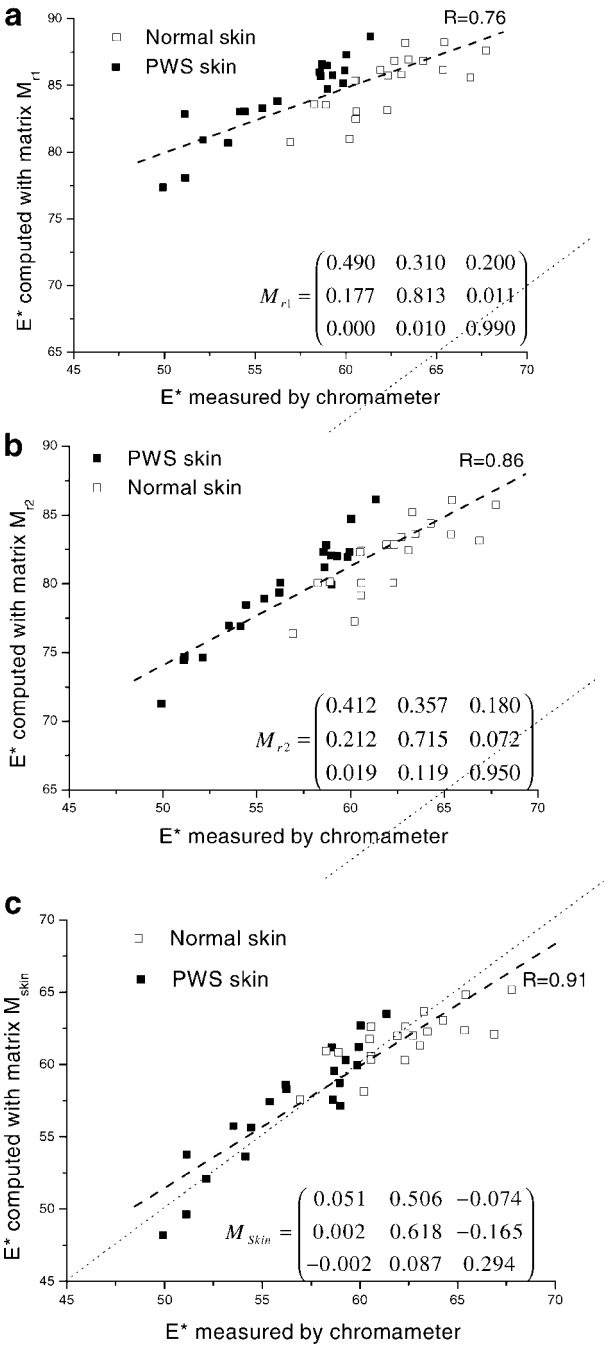

Fig. 3. Correlations between E^* parameters of normal and PWS skin sites measured with the chromameter and the CDR imaging system using (**a**) $\mathbf{M}_{r1}$, (**b**) $\mathbf{M}_{r2}$, and (**c**) $\mathbf{M}_{skin}$, respectively. The dashed lines are fits of the 40 data points with R of 0.76, 0.86, and 0.91, respectively, and the dotted line represents a perfect match between the CDR system and chromameter, for reference.

CONCLUSIONS

We used a cost function minimization algorithm to derive an optimized conversion matrix specific to our CDR color imaging system to transform the device-dependent RGB color space into the device-independent CIELAB color space. The presented conversion matrix is valid only as long as our specific camera and illumination conditions are preserved. Though some of the CDR color imaging components may be replaced during a long-term patient monitoring period, it is possible to keep comparable data without discontinuity when using the new conversion matrix to provide device-independent images. Use of the calibrated optimal matrix improves the utility of CDR color images as a simple non-contact measurement technique to monitor quantitatively PWS response to laser therapy.

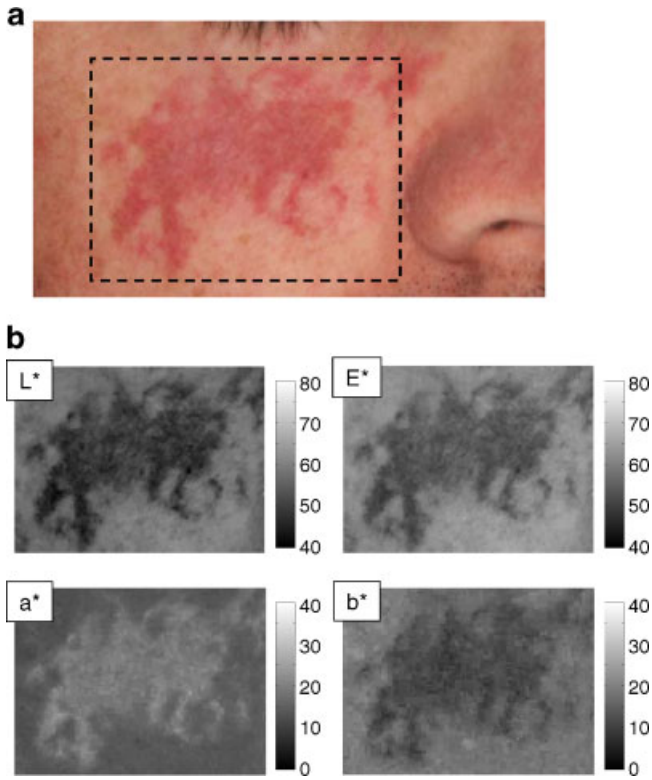

Fig. 4. **a**: RGB image of PWS skin taken with the CDR color imaging system. **b**: CIE color space images obtained using the CDR imaging system and $\mathbf{M}_{skin}$ on the PWS skin sites in (**a**). [Figure can be viewed in color online via www.interscience.wiley.com.]

ACKNOWLEDGMENTS

The work was supported in part by the Arnold and Mabel Beckman Fellows Program (B.C.), and NIH grants AR47551, AR48458, and EB002495 (J.S.N.).

REFERENCES

1. Nieman H. Pattern analysis and understanding, 2nd edn. Berlin/Heidelberg, Germany: Springer. 1990:22.
2. Haeghen YV, Naeyaert JMAD, Lemahier I. An imaging system with calibrated color image acquisition for use in dermatology. IEEE Trans Med Imaging 2000;19:722–730.
3. Koster PHL, Horst CMVD, Bossuyt PMM, van Gemert MJC. Prediction of portwine stain clearance and required number of flashlamp pump pulsed dye laser treatments. Lasers Surg Med 2001;29:151–155.

4. Verkruysse W, Lucassen GW, van Gemert MJC. Simulation of color of port wine stain skin and its dependence on skin variables. Lasers Surg Med 1999;25:131–139.
5. Andersen PH, Nangia A, Bjerring P, Maibach HI. Chemical and pharmacological skin irritation in man—a reflectance spectroscopic study. Contact Dermatitis 1991;25:283–289.
6. Trolius AM, Ljungre B. Reflectance spectrophotometry in the objective assessment of dye laser-treated port-wine stains. Br J Dermatol 1995;132:245–250.
7. Serup J, Agner T. Colorimetric quantification of erythema—a comparison of two colorimeters (Lange micro color and Minolta chromameter CR 200) with a clinical scoring scheme and laser Doppler flowmetry. Clin Exp Dermatol 1990;15: 267–272.
8. Wyszecki G, Stiles W. Color science: Concept and methods, quantitative data and formulae, 2nd edn. New York: Wiley. 1982.
9. Barel AO, Clarys P, Alewaeters K, Duez C, Hubinon JL, Mommaerts M. The Visi-Chroma VC-100: A new imaging colorimeter for dermatocosmetic research. Skin Res Technol 2001;7:24–31.
10. Wu W, Allebach JP, Analoui M. Imaging colorimetry using a digital camera. J Imaging Sci Technol 2000;44:267–279.
11. Miyamoto K, Takiwaki H, Hillebrand GG, Arase S. Development of a digital imaging system for objective measurement of hyperpigmented spot on the face. Skin Res Technol 2002;8: 227–235.
12. Pointer MR, Attridge GG, Jacobson RE. Practical camera characterization for colour measurement. Imaging Sci J 2001;49:63–80.
13. Cunha DAD, Eadie LH, Barbur JL, Hawkes DJ, Seifalian AM. The effect of image colour distortion on evaluation of donor liver suitability for transplantation. Comput Biol Med 2004;34:615–632.
14. Nischik M, Forster C. Analysis of skin erythema using true-color images. IEEE T Med Imaging 1997;16:711–716.
15. Jung B, Choi B, Durkin AJ, Kelly KM, Nelson JS. Characterization of port wine stain skin erythema and melanin content using cross-polarized diffuse reflectance imaging. Lasers Surg Med 2004;34:174–181.
16. Jung B, Choi B, Shin Y, Durkin AJ, Nelson JS. Determination of optimal view angles for quantitative facial image analysis. J Biomed Opt 2005 (in press).
17. Westland S, Ripamonti C. Computational colour science using MATLAB. West Sussex: Wiley; 2004.
18. Takiwaki H, Miyaoka Y, Kohno H, Arase S. Graphic analysis of the relationship between skin colour change and variations in the amount of melanin and hemoglobin. Skin Res Technol 2002;8:78–83.